# ELASTO-PLASTIC BEHAVIOUR OF  A WARRINGTON-SEALE ROPE: EXPERIMENTAL ANALYSIS AND FINITE ELEMENT MODELLING

V. Fontanari, M. Benedetti

*University of Trento, Dipartimento di Ingegneria industriale, Via Sommarive, 9 – 38123 Trento (Italy), e-mail: vigilio.fontanari@unitn.it, matrteo.benedetti@unitn.it*

B.D. Monelli

*University of Pisa, Dipartimento di Ingegneria Civile e Meccanica, Largo Lucio Lazzarino- 56126 Pisa (Italy), e-mail: bernardo.monelli@ing.unipi.it*

**Abstract**

The mechanical behavior of Warrington-Seale (WS) strands as well as of a Warrington Seale rope with a polymeric fiber core is investigated. Specifically, the elasto-plastic response under axial loading conditions beyond the elastic limit is studied. Tensile tests were carried out on both WS strands and ropes. The strain-stress curves of single wires with different diameters were determined and used as input of a fully parametric Finite Element (FE) study aimed at investigating the stress and strain evolution in the rope in the elastic as well as in the elasto-platic regime. The numerical simulations, validated on the basis of the experimental results, are useful to shed light on the way the load is distributed among the wires. The different damage evolution and the most likely failure mechanisms of strands and of ropes were identified. Helpful remarks are drawn about the structural response of these components under heavy loading conditions.

**Keywords**: Wire rope with independent core, Warrington-Seale strand, elasto-plastic behaviour, damage mechanisms, nonlinear FEA.

# 1. INTRODUCTION

The ability to withstand high axial loads coupled with high flexibility, compactness and high strength to weight ratio have determined the success of ropes as structural elements for many applications. For this reason, a great effort has been devoted in the past century to develop theoretical models for the structural analysis and to build up experimental data bases necessary for explaining their mechanical behaviours. The structural complexity and the expensive experimental investigation together with the non-linear nature of the problem render the analysis particularly difficult, thus hindering the formulation and closed-form solution of the equilibrium equations of each wire. The knowledge of the state of internal stress could play a crucial role since it could allow not only to properly design the rope in relation to the external loads, but also to prevent some of the damage phenomena, such as the wear of the wires, which might be very detrimental to its functionality. In this context, some aspects of their mechanical response such as for example the way the plastic deformation spreads across the strand cross section beyond the elastic limit, so as to establish the damage evolution and predict rope's failure, have not been fully clarified yet.  In the literature, several analytical models have been published, the books of Costello [1] and Feyrer [2] summarise the theoretical foundations and also report a comprehensive database of experimental results. Theoretical models, based on a set of simplifying assumptions, provide an estimate of the stress state induced by external loads into the cross section of a single strand. As pointed out by Elata et al. [3] these analytical models can be grouped into two main categories: fiber-based approaches and rod-based approaches. The first ones consider the wires as fibres having axial stiffness without bending and torsion capabilities (e.g. Lanteigne [4], Cardoux and Jolicoeur [5]), the latter ones assume that wires behave like beams thus possessing not negligible flexural and torsional stiffness (e.g. Velinsky et al. [6], Costello and Miller [7], Costello [1]). Jolicoeur and Cardoux [8] compared theoretical predictions of different models with the results of experimental tensile tests showing that fibre-based models may provide a sufficiently correct representation for single strand. Of considerable interest for the development of a design methodology of multilay wire strands is the approach proposed by Velinsky [9] based on the formulation of a set of

dimensionless parameters, allowing the study of a wide variety fo strand configurations. For multistrand ropes the theoretical analysis is more complex Velinsky et al [6], Costello [1], Velinsky [10], adopted some simplifying assumptions to treat the wound strands starting from the formulation of the single multilay straight strand by incorporating the strands into the ropes in the same way as the single wire is incorporated into the single strand, thus predicting with satisfying approximation the rope's response. Utting and Jones [11,12] included in the analysis also contact deformation and friction effects among wires. Velinsky [13] extendend the design approach proposed in [9] to wire ropes with three types of cores, independent wire rope core, fiber core, wire strand core. For its versatility, this methodology showed to be effective for carrying out an optimization analysis in the strand design. Velinsky [14] showed the usefulness of this approach by carrying out an optimum design analysis formulated for rope's minimum weight. Raoff and Kraincanic [15] proposed an extension to multi-strand wire ropes of the orthotropic sheet theory initially developed for multilayer strands, thus allowing to estimate with fairly simples formulas wire ropes stiffness coefficients. In order to take into account the double helical geometry of the wound strands Wang and McKewan [16] proposed a geometrical modelling approach of strand's double helix configuration, necessary for a complete description of the load distribution among wires. An interesting application of this representation for multi strand constructions was proposed by Elata et al [3]. By considering the double-helix configuration of single wires (treated as fibres) within the wound strand they were able to relate the wire level of stress to the load applied to the rope, thus finding a good agreement between theoretical predictions and experimental results.

If, on the one hand, analytical models can be used to explain the behaviour of single wires and, in some instances, to qualitatively predict the mutual contact actions exchanged by the wires, they are unable to fully describe the mechanical response of the generic strand because of the various phenomena occurring simultaneously during in service loading, such as nonlinear contact condition, friction, plasticity and large displacements (full-slip regime vs. sticking conditions), which will inevitably affect the mechanical response. Some approaches based on the Finite Element analysis (FE) have been proposed to study these aspects in the last two decades. Chiang [17], Jiang et al. [18], Nawrocki and Labrosse [19] used the FE analysis to simulate a simple strand

made up of seven wires in order to investigate different aspects of the mechanical behavior such as for example the inter-wire motion, contact stresses and possible local plastic yielding. Jiang et al. [20] extended their analysis to a three layered straight wire strand by modeling a basic sector of the wire strand accounting for the helical symmetry. More recently, Fontanari et al. [21] presented a FE modelling and an experimental analysis of a full-locked rope undergoing a heavy thermal loading simulating a fire scenario. Imrak and Erdonmez [22] presented an interesting FE modelling of an independent wire rope core (IWRC) made up of six strands wound around a straight core strand. Stanova et al. [23,24] published a comprehensive work on the computer modelling of wire strands. They focused firstly on the development of a mathematical model able to generate any rope geometry and then carried out a FE analysis of a multi-layered strand. Moradi et al. [25] performed a finite element modelling of an independent core wire rope, made up of Warrington Seale strands, bent over a sheave, obtaining useful information for the failure analysis of the rope. Kmet et al. [26] used the approach proposed by Stanova et al [24] to study the mechanical behaviour of a four layered spiral strands bent over a curved support. They found very interesting information about the load sharing among wires.

Although these numerical models are computationally heavy, they provide results closer to the experimental evidences in estimating normal, torsional and flexural stiffness, if compared with predictions of analytical models and undoubtedly they could have an ever increasing impact on the study of these structural components.

Within this framework, the present work aims to develop a parametric numerical approach able to provide a complete and reliable description of the mechanical response beyond the elastic limit of wire strands and fiber-core wire ropes. The attention is firstly focused on the strand as this is the key component of strand ropes and then extended to the multi-strand fiber core rope. The capability of predicting the strand behaviour establishes the basis for the study of the structural response of the rope. Although, to date, various different types of strands have been developed and used in structural application, the Warrington-Seale constitutes by far the most widespread solution. This solution represents an optimal compromise between the high wear resistance of

Seale's configuration and the ability to withstand high loads together with high flexibility of the Warrington geometry.

The proposed FE parametric analysis has been developed with reference to this constructive solution, even if the FE model has been designed to be adapted to any strand's geometry. Experimental tensile tests were carried out on single wires to determine the material true stress and strain curve to be used in the FE model for predicting the strand behaviour. The FE model was set up on the basis of a sensitivity analysis and validated by comparing the predicted load vs. elongation curve with results of experimental tensile tests carried out on a 31-wires Warrington Seale strand and a six-stranded 186 wires rope with polymeric core. The numerical model was then used to evaluate the distribution of the load among wires at different steps of the test. In this way, the yielding mechanism and the plastic strain evolution responsible for the final failure both for the single strand and for the rope can be predicted.  .

## 2. GEOMETRY OF THE WARRINGTON SEALE STRAND AND OF THE FIBER CORE ROPE

The Warrington-Seale strand configuration and the corresponding standard wire's layers definition is represented in figure 1a. This solution consists of three concentric wire layers helically wound around the core wire, comprising a total of 31 wires having different cross section, aligned in a parallel configuration (the standard sequence labeling 12+6/6+6+1 reports the number of wires from the external layer to the inner core). This geometry is typically adopted for producing ropes to be used for ropeways and similar applications. The strand nominal cross-section amounts to nearly 143 mm$^2$ thus reaching an allowable breaking load around 240 kN.

The fiber core WS wire rope is made up of a polymeric core and 186 wires, subdivided into six 12+6/6+6+1 WS strand helically wound around the core. The geometry of the rope is represented in fig. 1b. Table 1 lists the main geometric-constructive features of the strand and of the rope.

Table 1. Warrington-Seale strand and rope: main geometric-constructive features.

| Strand | | | | |
|---|---|---|---|---|
| Wires | Wire diameter (mm) | | Nominal diameter (mm) | 13.5 |
| 1 | 2.06 | | Helical pitch (mm) | 115 |
| 6 | 1.92 | | Average Helix angle | 70° |
| 6/6 | 1.56/2.02 | | Breaking load (kN) | 244 |
| 12 | 2.70 | | | |
| Rope | | | | |
| Strands configuration | | | WS (12+6/6+6+1) | |
| Nominal diameter (mm) | | | 38 | |
| Strands Helical pitch (mm) | | | 273 | |
| Wires Helical pitch in the strand (mm) | | | 91 | |
| Breaking Load (kN) | | | 1390 | |



a)

Third layer,

First layer

Core wire

Second layer

Polymeric core

WS strand

12+6/6+6+1

b)

Figure 1. Schematic representation of the Warrington-Seale (WS 12+6/6+6+1) strand (a) and of the polymeric core Warrington-Seale rope made up by six WS wires strands (b).

## 3. EXPERIMENTAL CHARACTERIZATION

The wires were produced by cold drawing starting from high carbon steel C80 bars characterised by a pearlitic microstructure typical of nearly eutectoid steels. The nominal chemical composition is reported in Table 2.

Table 2. nominal chemical composition of C80 steel used for steel wires

| | C | Mn | Si | S | Cu | Sn |
|---|---|---|---|---|---|---|
| Wt% | 0.80-0.85 | 0.40-0.85 | 0.1-0.3 | <0.3 | <0.15 | <0.15 |

## 2.2. Tensile properties of the different wires

The wires constituting the WS strand are characterised by different cross sections (Table 1). The mechanical behavior of the wires are closely related to their degree of drawing (Fontanari et al. [27], Panteghini and Genna  [28], Phelippeau et al [29]). In order to account for this size effect, twelve specimens having length of 200 mm were prepared for each wire diameter. Tensile tests were carried out on an universal servo-hydraulic machine (Instron 8506 – 100 kN),  measuring elongation with an extensometer having a gauge length equal to 12.5 mm and an excursion of 2.5 mm with accuracy of 0.001 mm. Tests were carried out in position control with a crosshead speed of 1 mm/min at room temperature. The average representative σ-ε curves are shown in Figure 2, whereas principal tensile parameters are reported in Table 3.
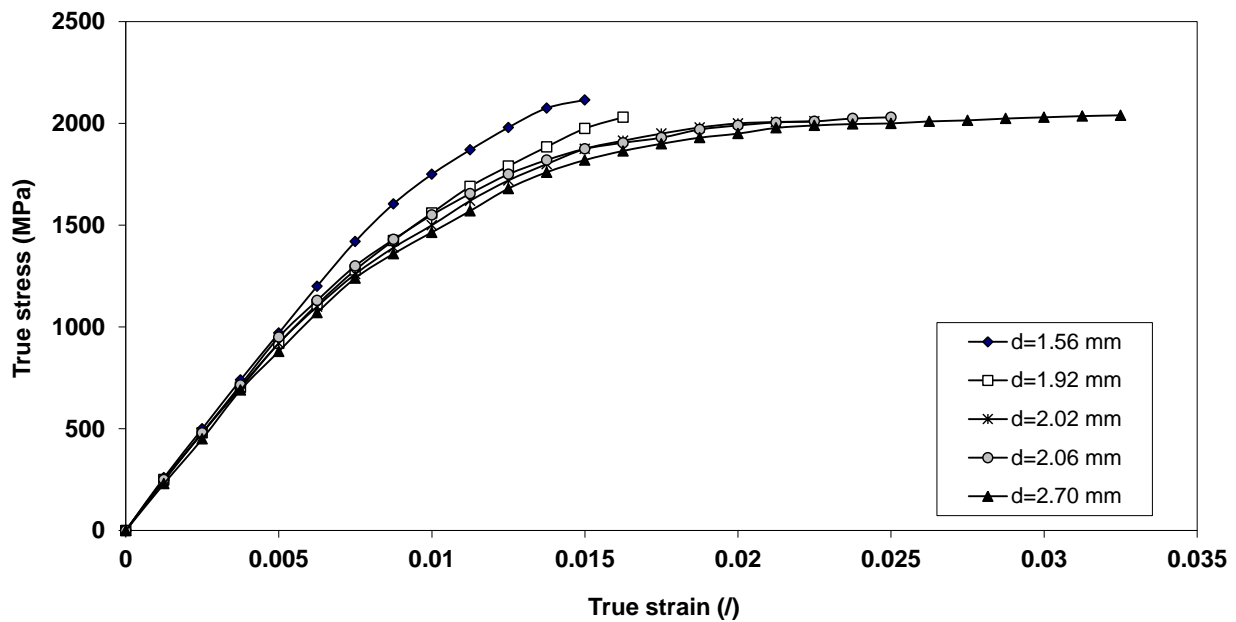


Figure 2: stress strain σ-ε curves of the different wires

Table 3. tensile properties of the different wires (mean values and 2 standard deviations interval)

| Wire diameter (mm) | Young Modulus (GPa) | Yield strength (MPa) | Tensile strength (MPa) | Elongation at fracture (%) |
|---|---|---|---|---|
| 2.06 | 196 ±15 | 1391±25 | 2025 ±15 | 2.3 ±0.4 |
| 1.92 | 203 ±10 | 1505±21 | 2045 ±45 | 1.4 ±0.25 |
| 1.56 | 198±11 | 1646±20 | 2120 ±55 | 1.4 ±0.25 |
| 2.02 | 202 ±10 | 1395±20 | 2040 ±20 | 2.3 ±0.3 |
| 2.70 | 200±12 | 1351±35 | 2020 ±10 | 3.3 ±0.3 |

As expected, the extent of cold drawing affects the tensile properties of the wires. In fact, the wires with the highest diameter, belonging to the external (first) mantle, show an appreciable elongation at fracture, whereas wires having smallest diameters belonging to the second and inner (third) layer, due to the intense cold working, show a very limited plastic deformation at fracture along with more scattered values of tensile strength and elongation at fracture. The core wire displays an intermediate behaviour.

## 2.3. Tensile behaviour of the Warrington-Seale strand and rope

The load vs. elongation curves were determined on a Instron DYNS 10MN testing machine equipped with a 1MN load cell for the WS strand and 10 MN load cell for the strand rope. Tests were carried out at Latif laboratories following a procedure conformal with standard specification, which involves the application of six loading-unloading cycles up to a load of nearly one half of the predicted fracture load. This procedure is necessary in order to compact and align the wires. In this way, in the seventh cycle a more realistic value of the in service elastic modulus can be determined. Specimens having a length equal to 4000 mm have been prepared. Elongation was measured over a length ($L_0$) of 1000 mm with an LVDT transducer having an excursion of 100 mm with an accuracy of 0.001 mm. Three tests and one test were carried out respectively for the strand and for the rope. Specimens were not taken to rupture in order to preserve the integrity of the extensometer. Figure 3 and 4 show the nominal stress (applied load over nominal cross section) vs. nominal strain curves respectively for the strands and the rope. The strand has a linear response, characterized by an elastic modulus equal to 175 ± 6 GPa, up to a load of around 120 ±10 kN (nominal stress of about 800 MPa). Beyond this value, a progressive deviation from linearity can be observed. A previous preliminary test carried out without mounting the extensometer returned a value of 244 kN as strand's breaking load. The three instrumented tests on the WS strands were then carried out up to a load of nearly 205 kN, which correspond to about 85% of the breaking load. For the WS rope, following the initial rope's cyclic adjustment, an elastic modulus of 138 GPa

can be estimated. In this case the test was interrupted at about 75% of the estimated rope's breaking load.
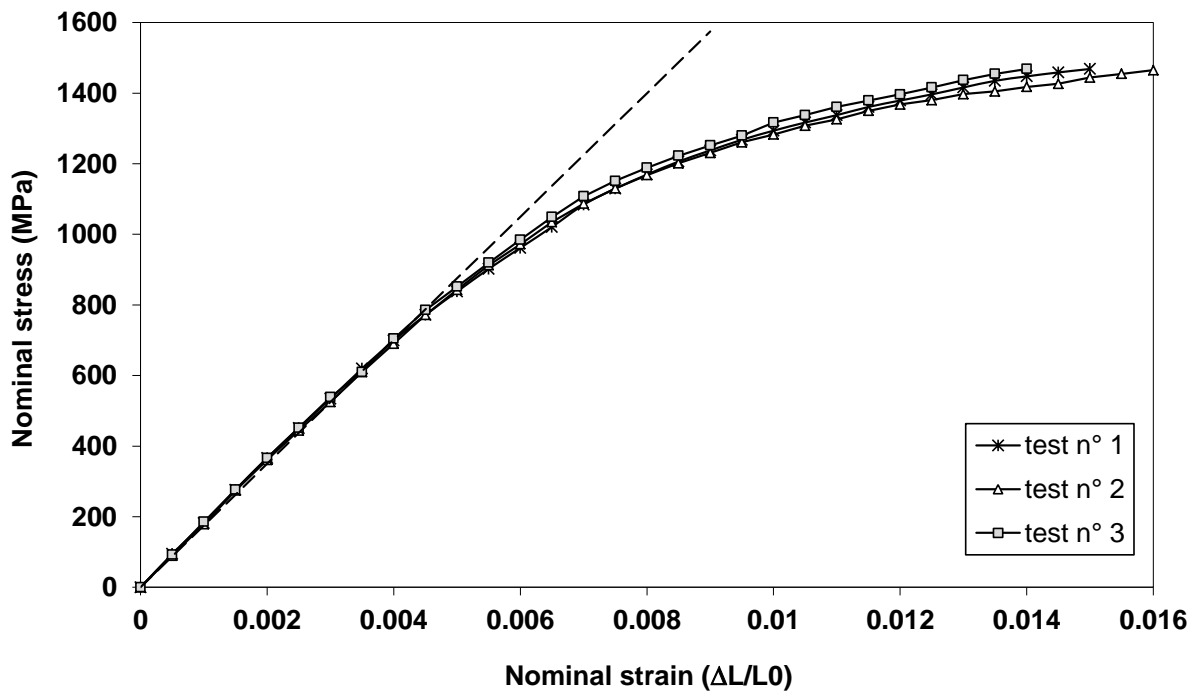


Figure 3. Nominal stress vs. nominal strain curves of the Warrington-Seale strands.
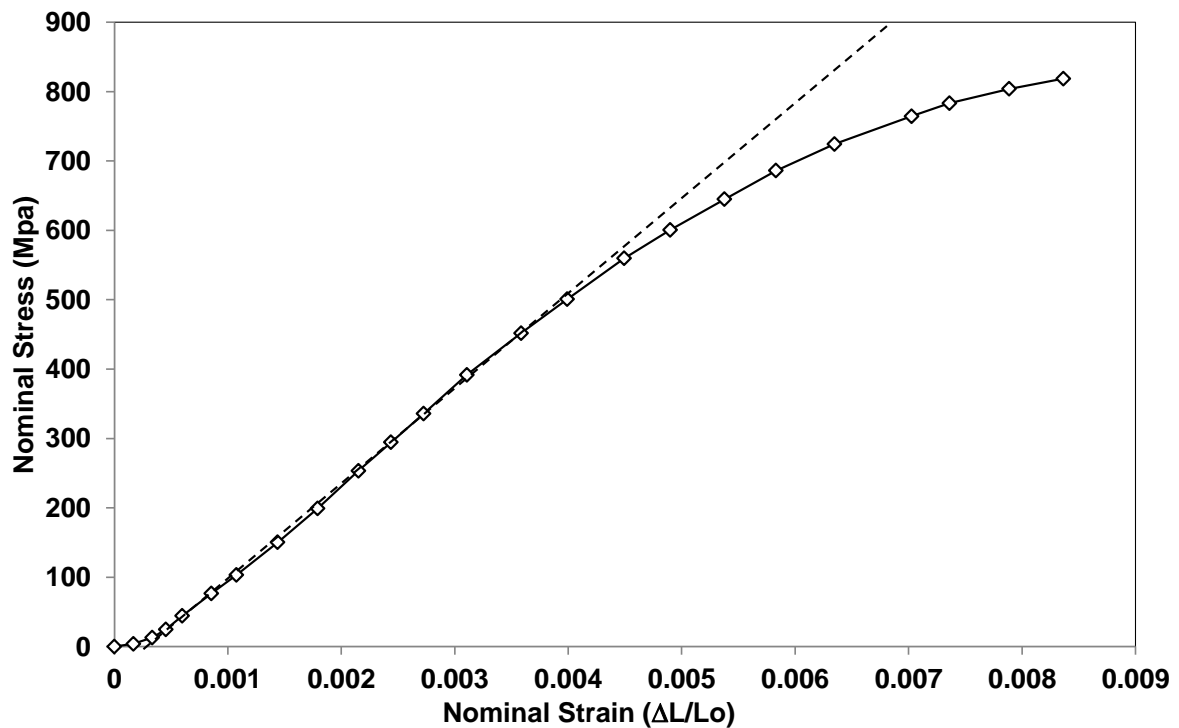


Figure 4. Nominal stress vs. nominal strain curve of the WS-rope with fiber core.

# 3. FINITE ELEMENT MODELING OF THE STRAND AND ROPE STRUCTURAL RESPONSE

The strands currently used for structural applications are usually characterized by a complex configuration making it very difficult to predict the structural response by adopting analytic approaches. This difficulty is even clearer for ropes made up of strands wound around a polymeric core, due to the double helical configuration of the wires. The basic assumptions are in fact highly restrictive even for predicting the elastic behaviour and are useless to investigate the damage mechanisms characterizing the component behaviour after the plastic deformation process has been triggered. The study can be faced by developing a Finite element model able to account for the nonlinear response of the structural part, due to wires contact and material plastic deformation.

## 3.1. Finite Element Modeling

The FE model has been developed to predict the response under conditions of purely axial load as well as axial load and torsional actions. Taking into account the torque associated with the unwinding tendency of the wires, each section of a flexible subjected to pure axial action undergoes a displacement field characterized by only two components different from zero: the principal one in the longitudinal direction and the other in the radial direction, as a consequence, the circumferential displacement must be constrained. The conceptual scheme for boundary and loading conditions of the FE model is shown in Figure 5 for the WS strand. A similar strategy has been adopted also for the WS-rope by treating the strands as wires in the single strand.

**Axial displacement**

**Axial displacements constrained**

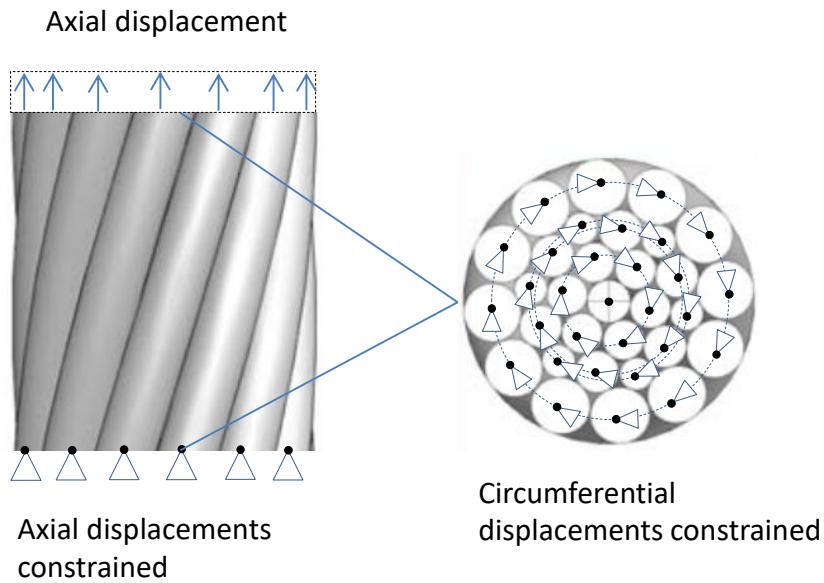**Circumferential displacements constrained**

Figure 5. Conceptual scheme of boundary and loading conditions

By considering the geometric complexity that characterizes this type of systems and in particular the high number of wires that have to be discretized, the feasibility of the numerical analysis depends strongly on the overall dimensions of the model, which must be kept below a reasonable value. For this purpose, a preliminary analysis was performed on simpler components (strand 6+1), aimed at determining the minimum longitudinal dimension of the overall model above which the edge effects do not affect the mechanical response anymore. The model qualification for the 6+1 strand can be conducted by comparing its predictions with those provided by the theoretical model of Costello [1]. This analysis showed that edge effects can be neglected for a longitudinal length at least equal to 1/20 of the strand helical pitch. The value of 1/16 was assumed for the present analysis.

The modelling approach has been designed in such a way that, once the geometric parameters have been defined, the model can be implemented either within the preprocessor of the FE code or via solid modeling with external software. FE analysis was carried out by using the Ansys rel. 12 commercial code. Brick 8-node elements were used for meshing the volumes. The obtained FE mesh for the WS strand and a detail on the mesh terminal section are shown in figure 6. The discretization used for modelling the six-stranded rope is similar. It has to be pointed out that the principal function of the polymeric core is to support the strands and to avoid their contact during load-

ing, a simplified volume meshed by brick 8-node elements was created to simulate this bearing effect. The FE model of the rope is shown in figure 7.
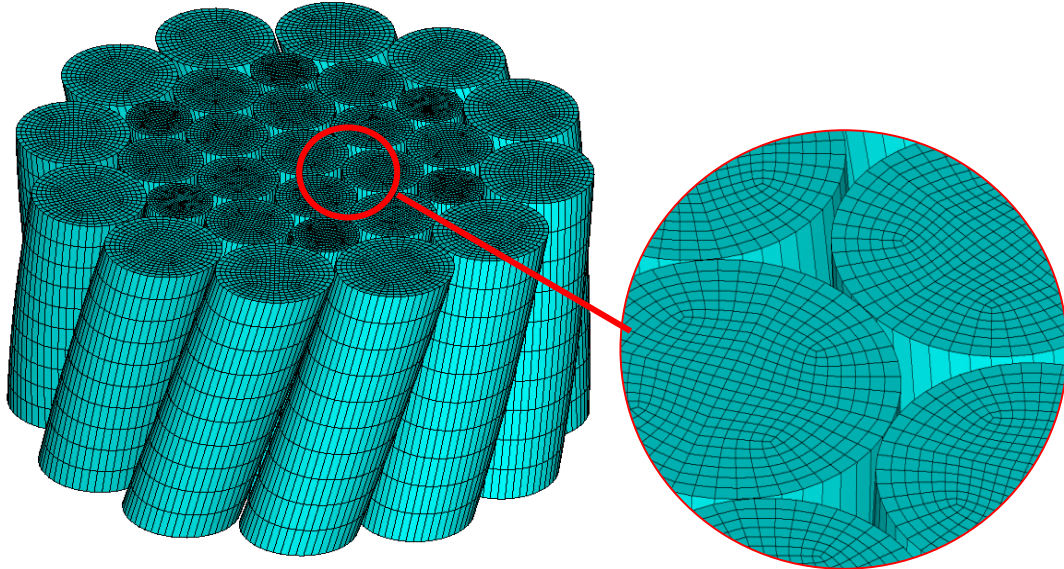


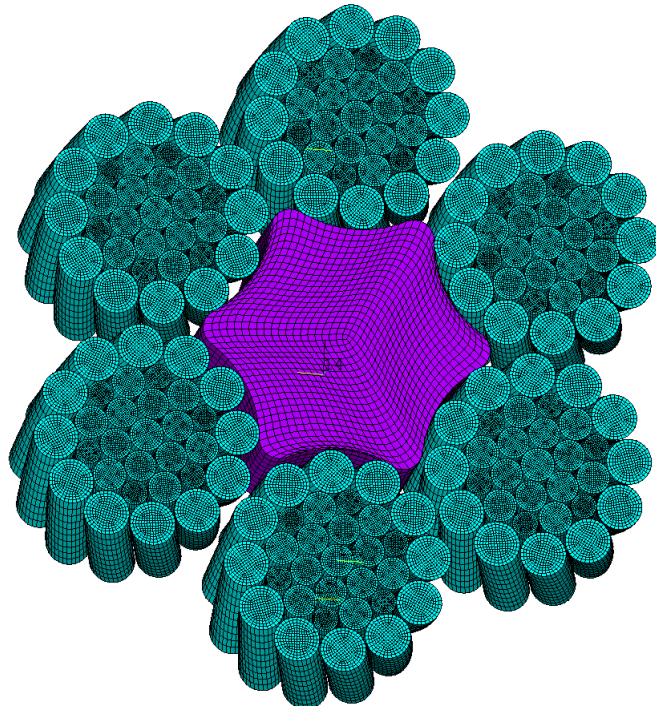Figure 6. a) FE mesh; b) detail of the mesh at terminal section 2.



Figure 7. FE mesh of the 6-stranded rope

The choice of element dimensions along the longitudinal and radial directions was based on an appropriate sensitivity analysis which showed that the predicted global response of the strand can be considered mesh independent by using 8-node three-dimensional structural elements having a

characteristic radial dimension at least equal to 1/12 of the wire radius and a longitudinal length lower equal to 1/10 of the axial span. The contact among wires has been modelled by surface-surface to 4 nodes contact elements, implementing the Augmented Lagrange multipliers approach in order to minimize the effects of normal contact stiffness and to minimize interference (Bathe [30]).

The results reported in the textbooks of Costello [1] and Feyer [2] show that for strands subjected to purely axial load conditions, the relative displacements between wires are practically negligible. It comes out that the friction does not play a significant role on the local stress-strain distribution, nevertheless for the present FE analysis the effect of friction was accounted for by introducing a Coulomb friction coefficient of 0.15.

Wire's material has been assumed as homogeneous, following the $J_2$ flow criterion and an isotropic hardening behavior and the incremental theory of plasticity. This assumptions are reasonable for metallic materials and in particular for steels also taking into account the monotonic loading conditions applied to the rope. To this purpose multilinear isotropic hardening (MISO) models were considered in the Ansys code by supplying, as tables of $\sigma-\varepsilon$ couples, the true stress-true strain curves obtained by the previously described experimental characterization, carried out for different wire sizes. The polymeric core was represented by a simplified bilinear isotropic hardening (BISO) model characterised by an elastic modulus of 1.6 GPa an Yield strength of 50 MPa and a plastic modulus of 160 MPa.

The axial loading conditions were simulated in order to reproduce on the wires, at the boundary terminal cross sections, the displacement field corresponding to a configuration of axial elongation. Following the conceptual scheme depicted in fig. 5, at terminal section 1, axial and circumferential displacements were constrained leaving radial displacements free, whereas on terminal section 2 an increasing axial displacement was applied maintaining the same constraint of section 1 for circumferential and radial displacements.

## 3.2. FE model validation

The validation of the model was conducted by comparing the numerical nominal stress vs. strain curves with the experimental ones. The results of this comparison can be appreciated in figure 8 and 9 respectively for the strand and the rope. The values of the elastic modulus and the deviation from linear behaviour obtained from the two approaches are collected in Table 4.

Table 4. Comparison of the characteristic properties of WS strand and rope

|        |                                |       | Experimental | Numerical |
|--------|--------------------------------|-------|--------------|-----------|
| Strand | Elastic Modulus                | (GPa) | 175          | 173       |
|        | Deviation from proportionality | (MPa) | 800          | 830       |
| Rope   | Elastic Modulus                | (GPa) | 138          | 134       |
|        | Deviation from proportionality | (MPa) | 540          | 575       |

The comparison shows that the FE model can reproduce with good approximation the experimental behaviour of both strand and rope. The relative differences are about 1% in predicting both the strands elastic modulus and proportionality limit. As regards the estimation of the axial stress as a function of the relative elongation the differences are always kept within 4%.

The good correspondence between the numerical results and experimental findings serves as validation of the FE analysis, which can therefore be used to explore how the load is distributed among the wires layers and to catch the onset of plastic damage as well as the causes that trigger it. The effect of the polymeric core on the tensile behavior is marginal and cannot be appreciated in the nominal stress-nominal strain curve of the rope. The material, indeed is characterized by an elastic modulus nearly two orders of magnitude lower than that of the strands, moreover the yield strength is nearly 1/25 of that of steel wires. . Therefore it does not contribute to a significant extent at sustaining the axial load but act primarily as a radial support of the strands, avoiding their mutual contact.
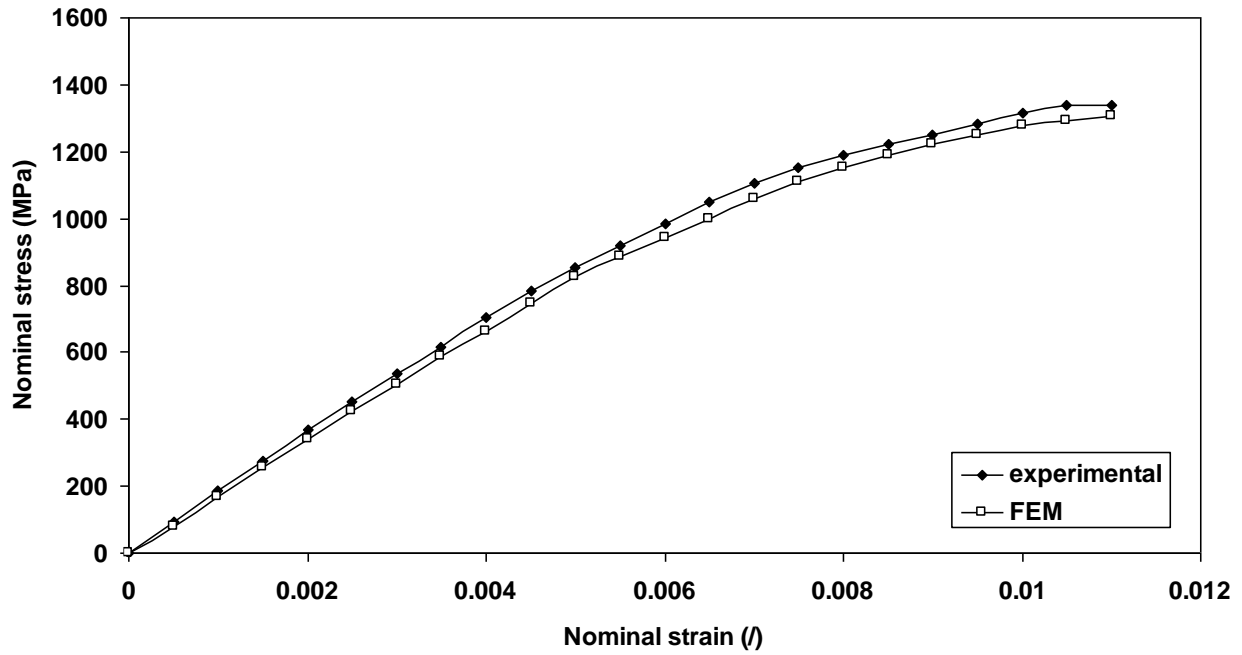
Figure 8. Comparison between the stress-strain curves obtained by FE and experimental test for the WS strand.
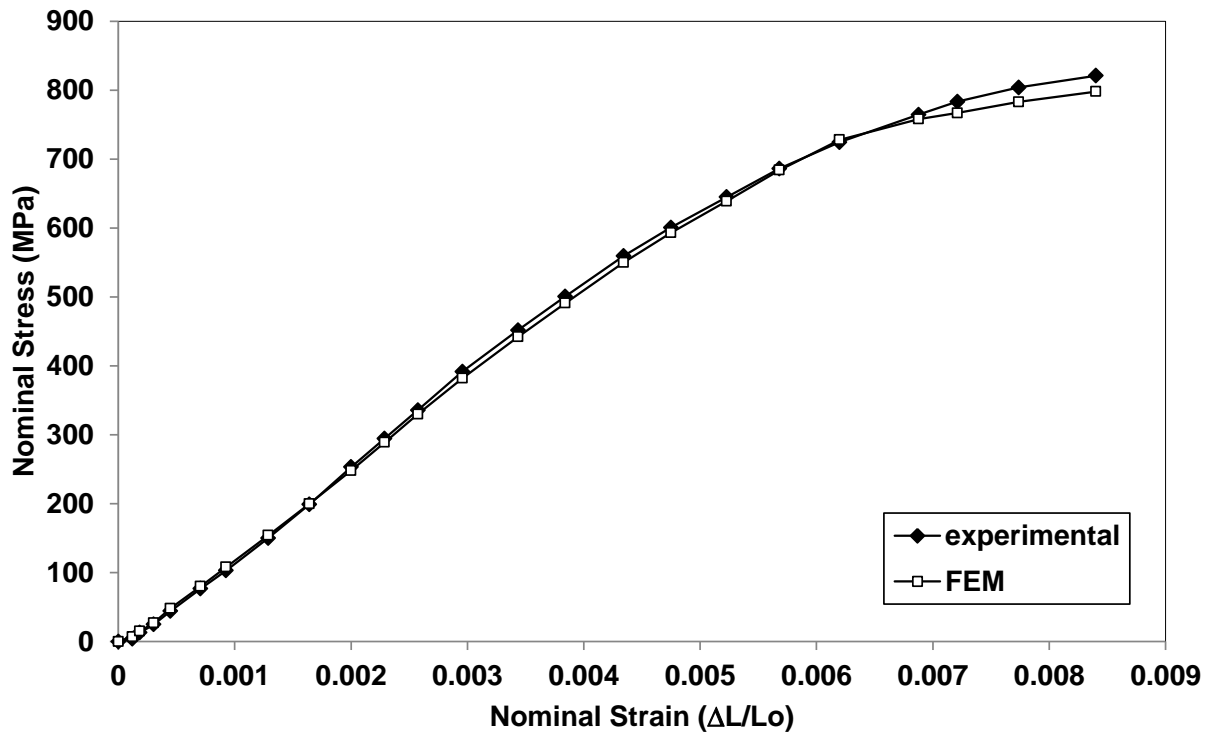


Figure 9. Comparison between the stress-strain curves obtained by FE and experimental test for the WS rope.

## 4. NUMERICAL RESULTS AND DISCUSSION

### 4.1. Stress and strain conditions in the wires of the WS strand

The nominal stress experienced by wires is plotted in figure 10 as a function of the strand nominal strain. Nominal stress is determined dividing the axial load calculated by FE in each wire by its cross section. Several observations can be drawn by analysing the stress values experienced by the different wire layers at increasing values of the strand nominal strain.. All the wire layers show a linear response up to a relative elongation of around 0.5%. At higher elongation values the wires start deviating from the linear behaviour due to the onset of plastic deformation. At elongation values above 0.6% the process of plastic deformation seems to have been extended to all the layers of the strand. The core wire and the third layer represent the stiffest paths, due to their alignment with the applied load direction. They therefore undergo higher stress conditions at every value of the nominal strand deformation. The onset of plastic deformation in the wire determines a stress redistribution thus involving the external wires to a major extent in carrying the applied load.
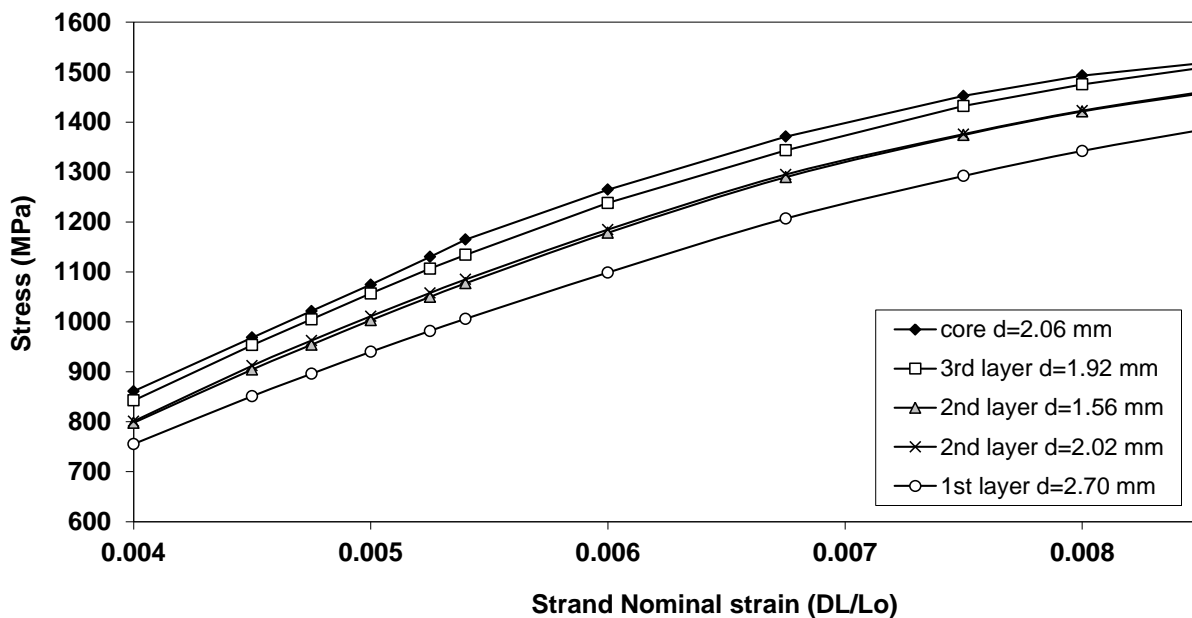


Figure 10. Evolution of wire's nominal stress vs. rope's nominal strain.

The axial load conditions cause a mutual approach between wires, which determines a state of multi-axial tension characterized by a radial component of compression and a tensile axial stress in the contact regions. Under these conditions, it has to be expected that materials yielding starts

developing along the helixes representing the contact areas as can be observed for the core wire in figure 11 that shows the equivalent plastic deformation produced at imposed elongations of 0.5% and 0.7%, respectively. A similar scenario can be identified for the other wire layers.
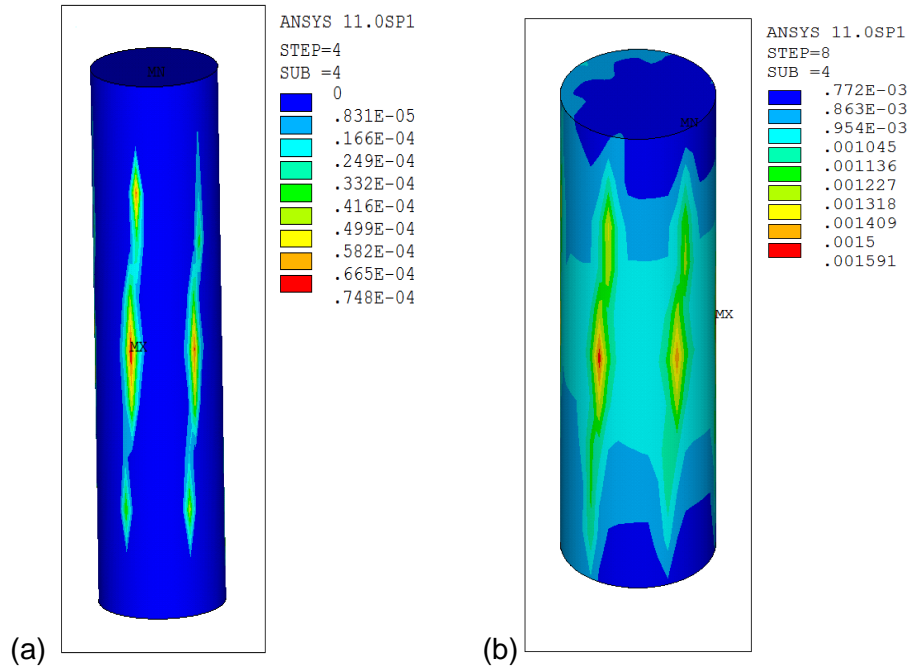


(a)                                             (b)

Figure 11. Evolution of the equivalent plastic strain in the core wire; strand relative elongation respectively of 0.5% (a) and 0.7% (b).

This damage scenario and the simultaneous load redistribution among wires can be confirmed by taking into account the evolution of plastic deformation at different stages of the axial elongation (Fig. 12). For an imposed relative elongation nearly equal to 0.5% (Fig. 12 (1)), the plastic deformation takes place along the contact helices mainly affecting the central wire, while only a small portion of wires belonging to the inner mantle seems to be involved in the plastic deformation process. By further increasing the elongation, the plastic flow spreads radially, gradually extending to the outer wire layers. Although the expansion of the plastic nucleus occurs very quickly, the values of plastic strain are quite small and heterogeneously distributed.
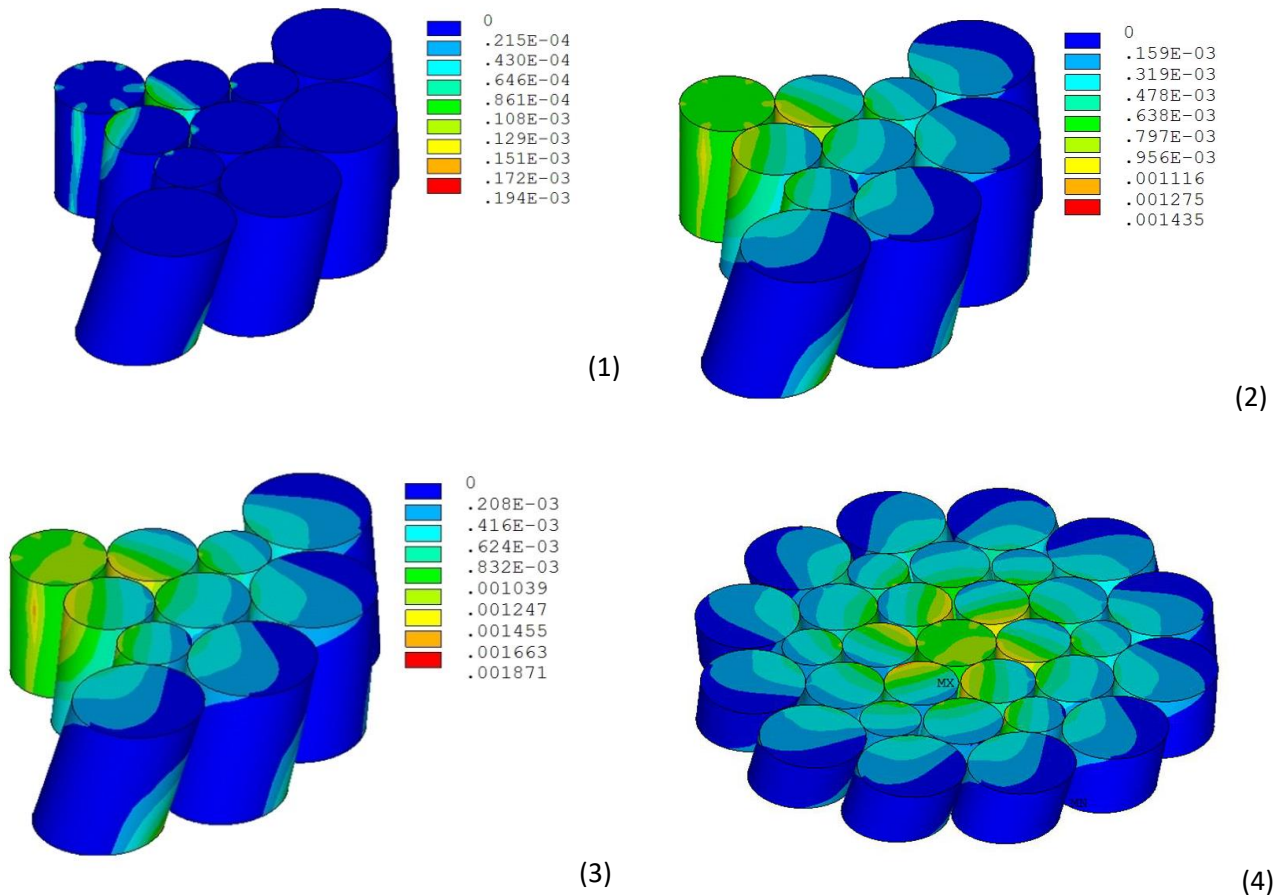
Figure 12. Evolution of the equivalent plastic strain in a generic cross section of the strand as a function of nominal strain: (1) 0.5%, (2) 0.7% and (3) 0.8%, (4) whole cross section at 0.8%

The plastic strain evolution is connected with load redistribution among wires. This aspect can be highlighted by considering the Stress Ratio (SR) between the stress determined for the single wire (see fig. 10) and the average stress calculated on the entire load bearing area (S.R.= $\sigma_{wire}/\sigma_{average}$). The obtained SR values are plotted vs. strand nominal strain in figure 13: the core wire in the elastic regime carries an increasing fraction of the total load. This can be explained considering that this wire is loaded along its axis, whereas the remaining wires, due to their helical configuration are bent thus getting a progressive alignment with the strand axis. At the onset of plastic deformation (fig 12 (1) and 13 (1)), the SR of the core wire starts decreasing thus pointing out a certain amount of load redistribution. This process goes progressively on as plastic deformation spreads across the strand section ( fig. 13 (2) and (3) and corresponding fig. 12 (2) and (3)), hence the SR of the outer layer increases progressively.
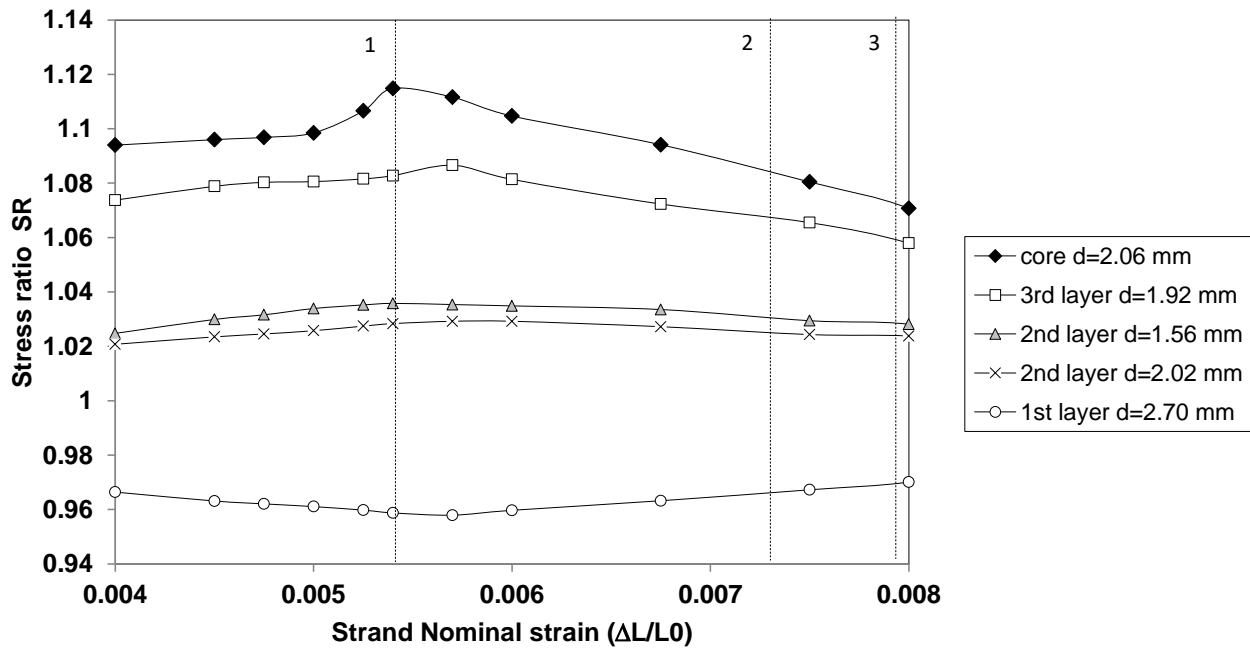
Figure 13. Stress Ratio (SR) vs. strand nominal strain.

## 4.2. Stress and strain conditions in the wires of the rope

The onset and the progressive spread of plastic deformation in the cross section of the strand belonging to the WS rope are represented in figure 14. The plastic strain originates eccentrically with respect to the strand section: the core wire is no more the critical wire as for the single WS strand. In this case, the position of the critical wire is shifted towards the center of the rope. Due to the double helix configuration of the strand, this wire represents the stiffest path for axial loading. By further increasing the axial load after plastic deformation, the plastic nucleus progressively spreads towards the center of the strand.

The material strain hardening and the different degree of work hardening experienced by the wires may indicate that the collapse of the strand as well as of the rope will not occur immediately after the gross yielding of the strand section. Noteworthy, during the test simulation, plastic strain tends to concentrate in the core of the strand. After yielding, the structural behaviour is dictated by the capability of wires to dissipate energy by plastic deformation. In this context, the wires with the smaller diameter will represent the weakest point of the strand since they are more work-hardened. However the external wire layer can act as a safety cage taking into account both the facts that its

load bearing area is nearly 57% or the total cross section and that the wires are characterised by the highest ductility.
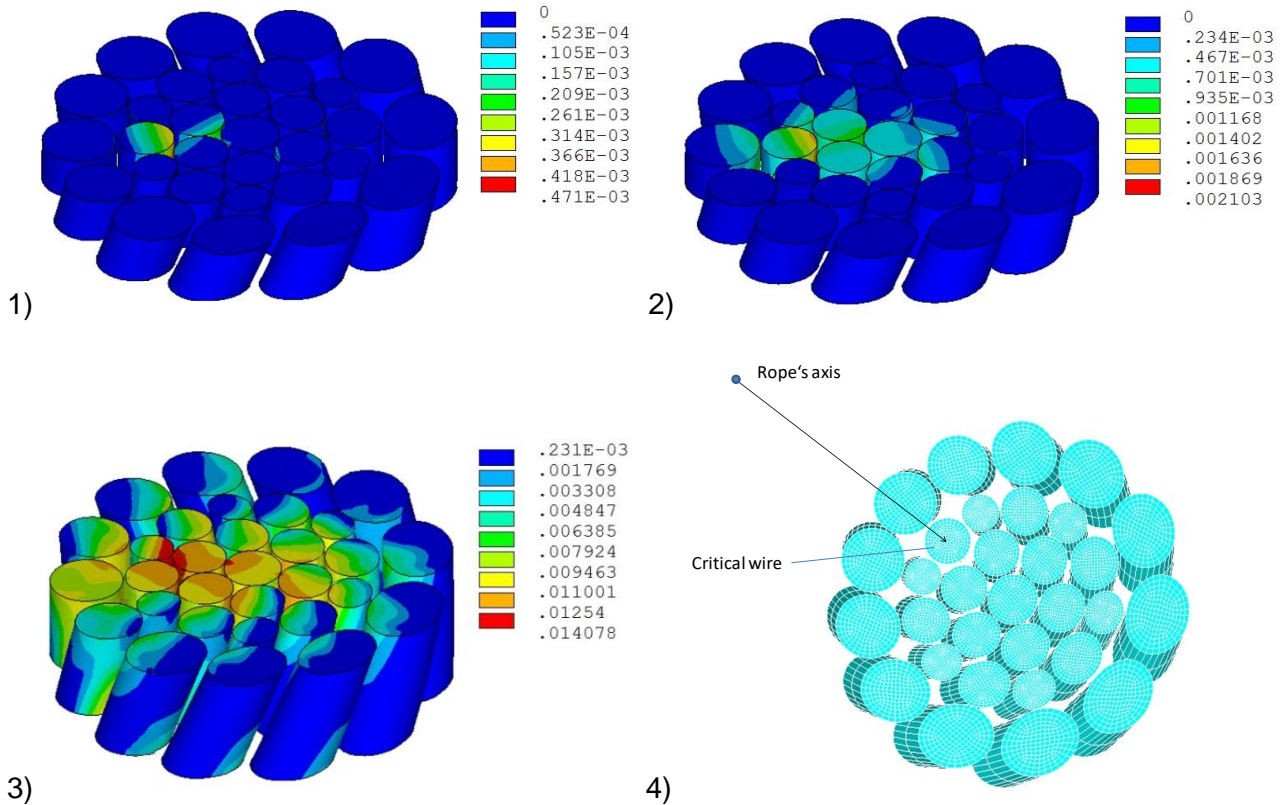


Fig. 14: Evolution of the equivalent plastic strain in a generic cross section of the strand as a function of rope's nominal strain: (1) 0.5%, (2) 0.65% and (3) 0.75%, (4) strand position with respect to rope's axis.

## 5. CONCLUSIONS

A FE fully parametric approach for evaluating the structural response of Warrington-Seale strands and ropes under axial loading was developed. The model was validated by comparison with the results of experimental tests. The load vs. elongation curves predicted by the numerical analysis showed a good agreement with those measured experimentally.

The FE model was then used to predict load redistribution among different wires and to determine the possible failure behaviour of the strand. It was found that in the elastic regime the load is not homogeneously shared among wires, due to the wires' helical configuration. For both strand and

ropes, the incipient plastic deformation is localised in the wires representing the stiffest path for the flow of axial loads. The onset of plastic deformation contributes to even out the load distribution among wires. The contact among wires plays a decisive role in the initiation of the plastic deformation process: i.e plastic deformation takes place along contacting helices. Yielding progressively involves the whole strand section, but thanks to the material strain hardening capability, the strand can withstand further increase in the applied load. Failure conditions are dictated by the different capability of wires to dissipate the mechanical work by plastic deformation.

**REFERENCES**

[1] Costello, G. A. (1997), "*Theory of Wire Rope*", Springer-Verlag.

[2] Feyrer, K., (2007), "*Wire Ropes. Tension, Endurance, Reliability*", Springer-Verlag.

[3] Elata,D., Eshkenazy,R., Weiss, M.P.,(2004) "*The mechanical behaviour of a wire rope with an independent wire rope core*", Int. J. of Solids and Structures, 41, 1157-1173.

[4] Lanteigne, J., (1985), " *Theoretical estimation of the response of helically armored cables to tension, torsion and bending*", Journal of Applied Mechanics, 52, 423-432.

[5] Jolicoeur, C., Cardou, A.,(1996), "Semicontinuous mathematical model for bending of multilayered wire strands", J. Eng. Mechanics, Div.ASCE, 122(7), 643-50.

[6] Velinsky, S. A., Anderson, G. L., Costello, G. A., (2001). "*Wire rope with complex cross sections*", J. of Engng. & Mech. , Div. ASCE, 110, 380-391.

[7] Costello, G. A., Miller, R. E., (1979), "*Lay effect of wire rope*", J. Engng. & Mech., Div. ASCE, 105, 4,597-608.

[8] Jolicoeur, C., Cardou, A.,(1991), " *A numerical comparison of current mathematical models of twisted wire cables under axisymmetric loads*", J. Energy Res. Tech., 113, 241-249.

[9] Velinsky, S. A.."Design and Mechanics of Multi-Lay Wire Strands", J. of Mechanisms, Trasmissions and Automation in Design, Trans. ASME, 110,June 1988, 152-60

[10] Velinsky, S. A. "Analysis of fiber core wire rope", J. of Energy Resources Technology, Trans. ASME, 107, Spetember 1985, 388-93

[11] Utting, W.S., Jones, N., (1987), "The response of wire rope strands to axial tensile loads, part I", Int. J. of Mechanical Sciences, 29 (9), 605-19.

[12] Utting, W.S., Jones, N., (1987), "The response of wire rope strands to axial tensile loads, part II", Int. J. of Mechanical Sciences, 29 (9), 621-36.

[13] Velinsky, S. A."On the design of Wire Rope", J. of Mechanisms, Trasmissions and Automation in Design, Trans. ASME, 111,September 1989, 382-88

[14] Velinsky, S. A. "A Stress Based Methodology for the Design of Wire Rope Systems", J. of Mechanical Design, Trans. ASME, 115, march 1993, 69-73

[15] Raoof, M., Kraincanic, I., (1995), "Analysis of large Diameter Steel Ropes", Journal of Engineering Mechanics, 121, 667-675.

[16] Wang, R. C., McKewan, W. M.,(2001), "*A model for the structure of round-strand wire ropes*", O.I.P.E.E.C. Bulletin, 81, 15-42.

[17] Chiang, Y. J., (1996), "Characterizing simple-stranded wire cables under axial loading". Finite Elements in Analysis and Design, 24, 49-66

[18] Jiang, W. G., Yao, M. S., Walton, J. M.,(1999), "*A concise finite element model for simple straight wire rope strand*", International Journal of Mechanical Sciences, 41, 143-161.

[19] Nawrocki, A., Labrosse, M., (2000), "*A finite element model for simple straight wire rope strands*", Computers and Structures, 77, 345-359.

[20] Jiang, W. G. , Henshall, J. L., Walton, J. M. (2000) "*A concise finite element model for three-layered straight wire rope strand*", International Journal of Mechanical Sciences, 42, 63-86.

[21] Fontanari, V., Monelli, B. D., Degasperi, F. (2009) "*Experimental and numerical analysis of locked coil ropes fire behavior*", Proceedings of 2009 SEM Annual Conference & Exposition on Experimental and Applied Mechanics, Albuquerque, New Mexico.

[22] ErdeM Imrak, C., Erdönmez, C.,(2010), "*On the problem of wire rope model generation with axial loading*", Mathematical and Computational Applications, Vol. 15, No. 2, pp. 259-268

[23] Stanova,E., Fedorko G., Fabian, M., Kmet, S., (2011), "Computer modelling of wire strands and ropes part I: Theory and computer implementation", Advances in Engineering Software, 42, 305-315.

[24] Stanova,E., Fedorko G., Fabian, M., Kmet, S., (2011), "Computer modelling of wire strands and ropes part II: Finite element-based applications", Advances in Engineering Software, 42, 322-331.

[25] Moradi,S., Ranjbar,K, Makvandi, H. (2012) ,"Failure analysis of a drilling wire rope", J Fail. Anal. And Preven., 12, 558-556

[26] Kmet, S., Stanova,E., Fedorko G., Fabian, Brodniansky,J.,(2013), "Experimental investigation and finite element analysis of a four-layered spiral strand bent over a curved support", Engineering structures, 57, 475-483.

[27] Fontanari, V., Bulf, U. , Benedetti, M., (2005)  "*Numerical analysis of the rolling process of shaped wires for locked steel ropes*", Journal of Material Processing Technology, 170, 97-107.

[28] Panteghini, A. , Genna, F. ,(2010), "Effects of the strain-hardening law in the numerical simulation of wire drawing processes" Computational Materials Science, 49,236–24

[29] Phelippeau, A., Pommier, S., Tsakalakos, T., Clavel, M., Prioul, C., (2006)  "Cold drawn steel wires—processing, residual stresses and ductility—part I: metallography and finite element analyses" Fatigue & Fracture of Engineering Materials & Structures, 29, (3), 201-207

[30] Bathe, K. J., (1996), "Finite Element Procedures", Prentice Hall.